

Estimation of Latent Heat Flux Using a Non-Parametric Method

Cheng-I Hsieh ^{1,*} , Cheng-Jiun Chiu ¹, I-Hang Huang ¹  and Gerard Kiely ²¹ Department of Bioenvironmental Systems Engineering, National Taiwan University, Taipei 10617, Taiwan² Civil and Environmental Engineering Department, Environmental Research Institute, University College Cork, Cork T12P2FY, Ireland

* Correspondence: hsieh@ntu.edu.tw; Tel.: +886-2-3366-3473

Abstract: The non-parametric (N-P) method expresses evapotranspiration as a function of net radiation, ground heat flux, air temperature, and surface temperature (T_s). This method is relatively new and attractive for estimating evapotranspiration, especially for T_s measurements from remote sensing. The purpose of this study is to investigate the limitations of this method and compare its performance with those of the Penman–Monteith (P–M) and Priestley–Taylor (P–T) equations. Field experiments were carried out to study the evapotranspiration rates and sensible heat fluxes above three different ecosystems: grassland, peat bog, and forest. The results show that above the grassland and peat bog, the evapotranspiration rates were close to the equilibrium evaporation. Though the forest is humid (average humidity $\approx 89\%$; annual precipitation ≈ 2600 mm), the evapotranspiration was only 69% of the equilibrium evaporation. In terms of model predictions, it was found that the P–M and P–T equations were able to predict the water vapor and sensible heat fluxes well ($R^2 \approx 0.60$ – 0.92 ; $RMSE \approx 30$ $W\ m^{-2}$) for all the three sites if the canopy resistance and the P–T constant of the ecosystem were given a priori. However, the N-P method only succeeded for the grassland and peat bog; it failed above the forest site ($RMSE \approx 60$ $W\ m^{-2}$). Our analyses and field measurements demonstrated that for the N-P method to be applicable, the actual evapotranspiration of the site should be within 0.89–1.05 times the equilibrium evaporation.



Citation: Hsieh, C.-I.; Chiu, C.-J.; Huang, I.-H.; Kiely, G. Estimation of Latent Heat Flux Using a Non-Parametric Method. *Water* **2022**, *14*, 3474. <https://doi.org/10.3390/w14213474>

Academic Editor: Alexander Yakirevich

Received: 29 September 2022

Accepted: 27 October 2022

Published: 30 October 2022

Publisher's Note: MDPI stays neutral with regard to jurisdictional claims in published maps and institutional affiliations.



Copyright: © 2022 by the authors. Licensee MDPI, Basel, Switzerland. This article is an open access article distributed under the terms and conditions of the Creative Commons Attribution (CC BY) license (<https://creativecommons.org/licenses/by/4.0/>).

Keywords: non-parametric method; Priestley–Taylor equation; Penman–Monteith equation; evapotranspiration

1. Introduction

Evapotranspiration (water vapor flux) is an important component of the water cycle, surface energy balance, and water resources. In order to accurately estimate water vapor fluxes, many methods have been developed [1,2]. Among them, the Penman–Monteith (P–M) equation [3] is the most widely used. However, the parameter in the P–M equation, canopy resistance, is needed a priori. Hence, the inconvenience and uncertainty of applying the P–M equation are having to parameterize the canopy resistance using primary meteorological data [4–6].

Priestley and Taylor proposed a simplified method, the Priestley–Taylor (P–T) equation, which mainly incorporates the effects of the unsaturated atmospheric demand term in the P–M equation into a single empirical constant [7,8]. Nevertheless, calibration for the empirical constant (Priestley and Taylor constant) is also necessary for successfully implementing the P–T equation [4,9,10].

To avoid the uncertainty caused by parameterization of canopy resistance in the P–M equation, Liu et al. [1] proposed a non-parametric (N-P) method based on Hamilton's principle [11] to estimate fluxes of water vapor (LE) and sensible heat (H). This method does not require empirical parameters, and directly uses the measured meteorological data as model inputs (i.e., net radiation, air temperature, ground heat flux, and surface temperature) to estimate surface fluxes. In their study, Liu et al. evaluated this method at 26 sites and found that 23 sites performed well, and even when compared to the P–M

equation and Bowen ratio method, the non-parametric method was found to perform best [1]. This method is particularly attractive for estimating LE with remote sensing data [12–15]. However, this method has not yet been tested over tall canopies (e.g., forests).

Yang et al. [16] evaluated the non-parametric method over two corn croplands and one bare soil site. They concluded that this method would overestimate water vapor flux under dry conditions and that use the non-parametric method in a dry environment should be avoided. Adopting this non-parametric method and using satellite data from a Moderate-Resolution Imaging Spectroradiometer (MODIS) and the China Meteorological Administration Land Data Assimilation System, Pan et al. [14] retrieved LE over an arid region and found that the LE was underestimated at all four sites. In addition, Pan et al. [12,13] showed that the non-parametric approach performed better above humid areas (e.g., wetland, vegetable site).

In summary, the non-parametric method is found to be unsuitable for arid environments but is still attractive for humid regions. Studies evaluating this method over humid conditions are still rare, especially for tall canopy environments (e.g., forests). The purpose of this study is to examine the non-parametric method above three different humid areas (grassland, peat bog, and montane forest) for estimating LE and H and compare its performance with two traditional methods: the P–M and P–T equations.

2. Experiments

Field experiments conducted over the three humid sites: grassland, peat bog, and montane forest, are described below.

2.1. Grassland

The grassland site is located approximately 25 km northwest of Cork in southern Ireland (59°59' N, 8°45' W; 195 m above sea level). This area has a rainy temperate climate with an annual average temperature of 9.4 °C and rainfall of 1207 mm. The annual average temperature during this study period (1 January 2013–31 December 2013) was 9 °C, mean humidity was 92%, and the annual rainfall was 1161 mm. This grassland site is a high-quality pasture and grassland, with perennial ryegrass as the main plant species, mixed with a small amount of foxtail grass and fluffy grass. Grass height was about 10–20 cm in pastures and up to 45 cm in grassland [17]. The average canopy height was 30 cm in year 2013. The soil type is gley with fertile soil, and the proportion of soil particle size is 42% sand, 41% silt, and 17% clay [18]. Soil organic carbon concentration was 5.9% in a 20 cm deep soil layer [19]. An eddy covariance (EC) system, which consisted of a CO₂/H₂O gas analyzer (Li-7500) and an ultrasonic anemometer (CSAT), was installed at 5 m above the ground. The sampling frequency and averaging period for this system were 10 Hz and 30 min, respectively.

Other measured meteorological data include net radiation (R_n), ground heat flux (G), air temperature (T_a), surface temperature (T_s), and relative humidity (RH). Soil thermometers were set up at 1.5, 5, and 7.5 cm below the ground, respectively. The measured frequency was one datum per minute, and the data was then averaged every 30 min. The site description and instrumentation are also summarized in Table 1. Additional experimental details can be found in Peichl et al. [20].

All of the three methods (P–M equation, P–T equation, N–P method) for estimating LE assume that the surface energy is closed (i.e., $R_n = H + LE + G$). For the purpose of this study, only data that satisfy the energy closure condition within 90% were selected. In other words, the difference between R_n and $H + LE + G$ should be within $\pm 10\%$. This data selection process was also applied to the other two sites (peat bog and forest). Figure 1 shows the scatter plots between R_n and H, LE, G, and $H + LE + G$. From Figure 1, we notice that in this grassland site, about 40% of the energy was used for warming the air (Figure 1a); 48% was distributed to evapotranspiration (Figure 1b); less than 10% of the energy was transported to the ground (Figure 1d); and the overall energy closure rate was about 97% after data

selection using the energy closure condition. These energy partition coefficients are also summarized in Table 2.

Table 1. Summary of site features and instrumental heights at the grassland, peat bog, and forest.

Site	Grassland	Peat Bog	Forest
Data period	1 January 2013–31 December 2013	1 January 2013–31 December 2013	22 May 2009–31 July 2010
Altitude (m)	195	150	1252
Location	59°59' N, 8°45' W	51°55' N, 9°55' W	23°39'51.09" N, 120°47'44.57" E
Climate type	Temperate	Temperate	Sub-tropical
Annual rainfall (mm)	1161	1834	2635
Mean temperature (°C)	9	10.1	16.6
Mean humidity (%)	92	82	89
Canopy height (m)	0.3	0.1	26
Surface emissivity	0.95	0.99	0.98
Canopy resistance ($s\ m^{-1}$)	60	63	134
Priestley–Taylor constant	0.962	0.956	0.692
Measurement height (m)			
Eddy covariance system	5	3	28
Air temperature & humidity sensor	5	3	28
Net radiometer	4	2	27.5
Soil heat flux plate	−0.1	−0.1	−0.05
Soil thermometer	−0.015, −0.025, −0.075	−0.1	−0.05, −0.1
Soil moisture meter	−0.05	−0.1	−0.05, −0.1

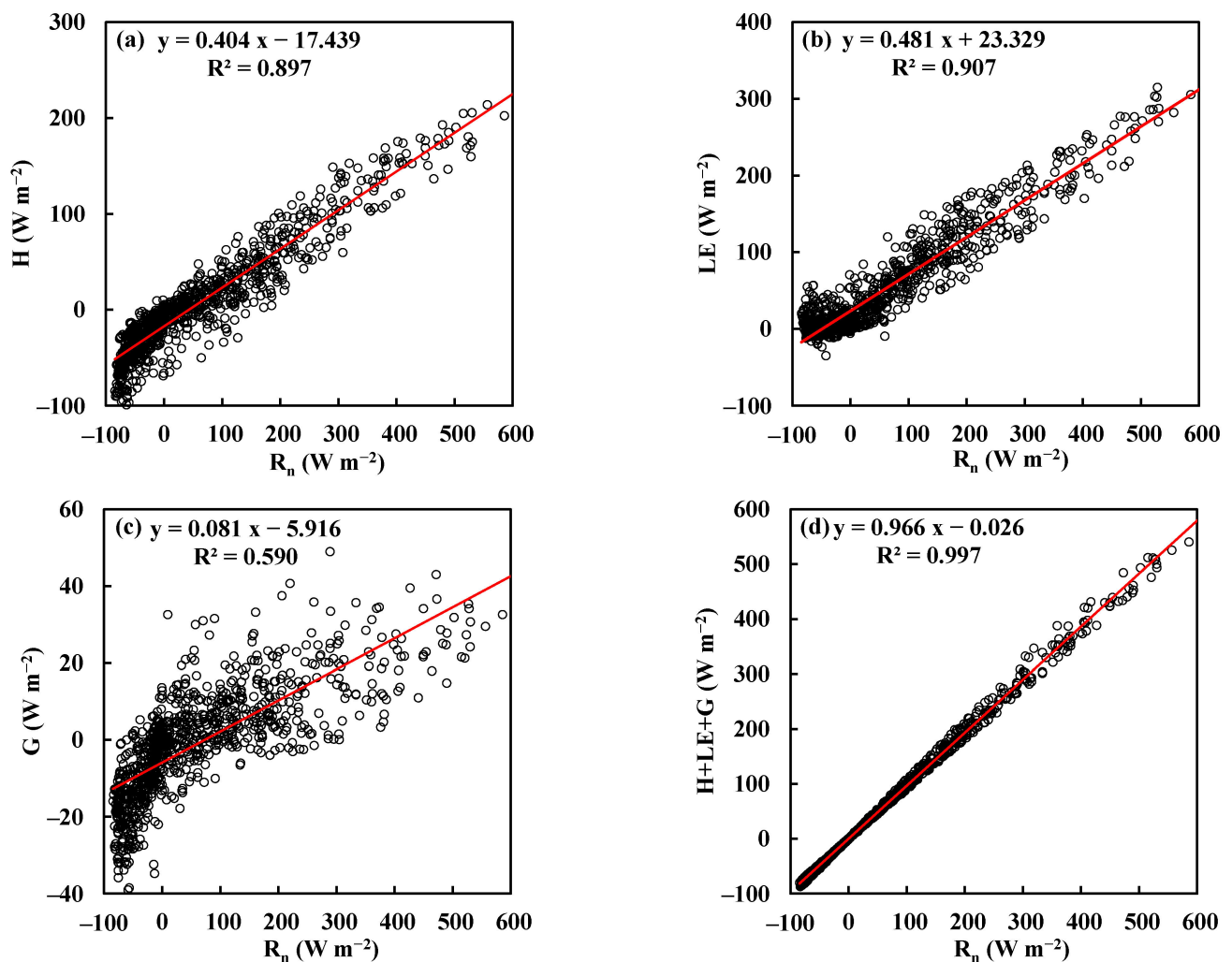


Figure 1. Scatter plots between R_n and H (a), LE (b), G (c), and H+LE+G (d) above the grassland.

Table 2. Summary of linear regression between R_n and H, LE, G, and H+LE+G for the grassland, peat bog, and forest sites. $Y = aX + b$; X is R_n ; Y is H, LE, and so on.

Flux	Grassland			Peat Bog			Forest		
	a	b	R ²	a	b	R ²	a	b	R ²
H	0.404	−17.439	0.897	0.426	−14.819	0.913	0.574	−14.495	0.893
LE	0.481	23.329	0.907	0.342	22.239	0.876	0.347	18.439	0.733
G	0.081	−5.916	0.590	0.210	−6.948	0.808	0.044	−3.459	0.474
H+LE+G	0.966	−0.026	0.997	0.977	0.472	0.997	0.965	0.485	0.997

2.2. Peat Bog

The peat bog site is an Atlantic blanket bog located at Glencar, County Kerry, south-west Ireland (51°55' N, 9°55' W, 150 m above sea level). This area also has a rainy temperate climate, with an average temperature of 10.1 °C, an average humidity of around 82%, and an annual rainfall of 1834 mm during the experimental period. In the center of the bog, the peat layer in the upper half consists mainly of reed sedge peat; the bulk density of the soil is 0.05 (g cm^{−3}), the porosity is 95%, and the depth of the peat layer varies from about 2 to 5 m [21]. In the southern part of the bog, there is a drainage river with a catchment area of 74 ha, of which about 85% of the surface is blanket peat, and the other 15% is grazing grassland and drained peat soils.

According to relative elevation, the landform of this site can be divided into four categories: hummocks (6%), high lawns (62%), low lawns (21%), and hollows (11%) [22]. Vascular plants and Bryophytes cover about 30% and 25% of the surface, respectively, in summers. The main species here are *Racomitrium lanuginosum* (Hedw.) Brid. and bog moss, in roughly equal proportions [23]. The average canopy height here was about 10 cm.

To measure fluxes of sensible heat, water vapor, and carbon dioxide, an eddy covariance system was installed at 3 m above the ground in the center of the peat bog. This EC system consisted of an ultrasonic anemometer (CSAT3) to measure three-directional wind speed and virtual potential temperature, and an open-path CO₂/H₂O infrared gas analyzer (Li-7500) to measure water vapor and carbon dioxide concentrations. The above variables were collected at a frequency of 10 Hz and averaged every 30 min. Additionally, air temperature and relative humidity were measured at 3 m above the ground; net radiation was measured by a net radiometer (CNR1) installed at 2 m. In addition, soil heat flux was measured 10 cm below the ground, and a soil thermometer was installed at the same depth to measure soil temperature. These measurements were collected every 1 min and averaged every 30 min [24,25]. This study uses data collected throughout year 2013. The site and instrumentation features are also listed in Table 1. Further experimental details can be found in McVeigh et al. [25].

Figure 2 plots the relationship between R_n and H, LE, G, and H+LE+G above this peat bog site. As seen in Figure 2, about 43% of the net radiation was used for warming the air and about 34% of the energy was distributed to evapotranspiration; 21% of the energy was transported to the ground; and the overall energy closure rate was about 98% after data selection using the energy closure condition. Compared with the grassland site, much more energy (21% vs. 8%) was directed into the ground due to a shorter vegetation canopy height. The regression analyses of Figure 2 are also listed in Table 2.

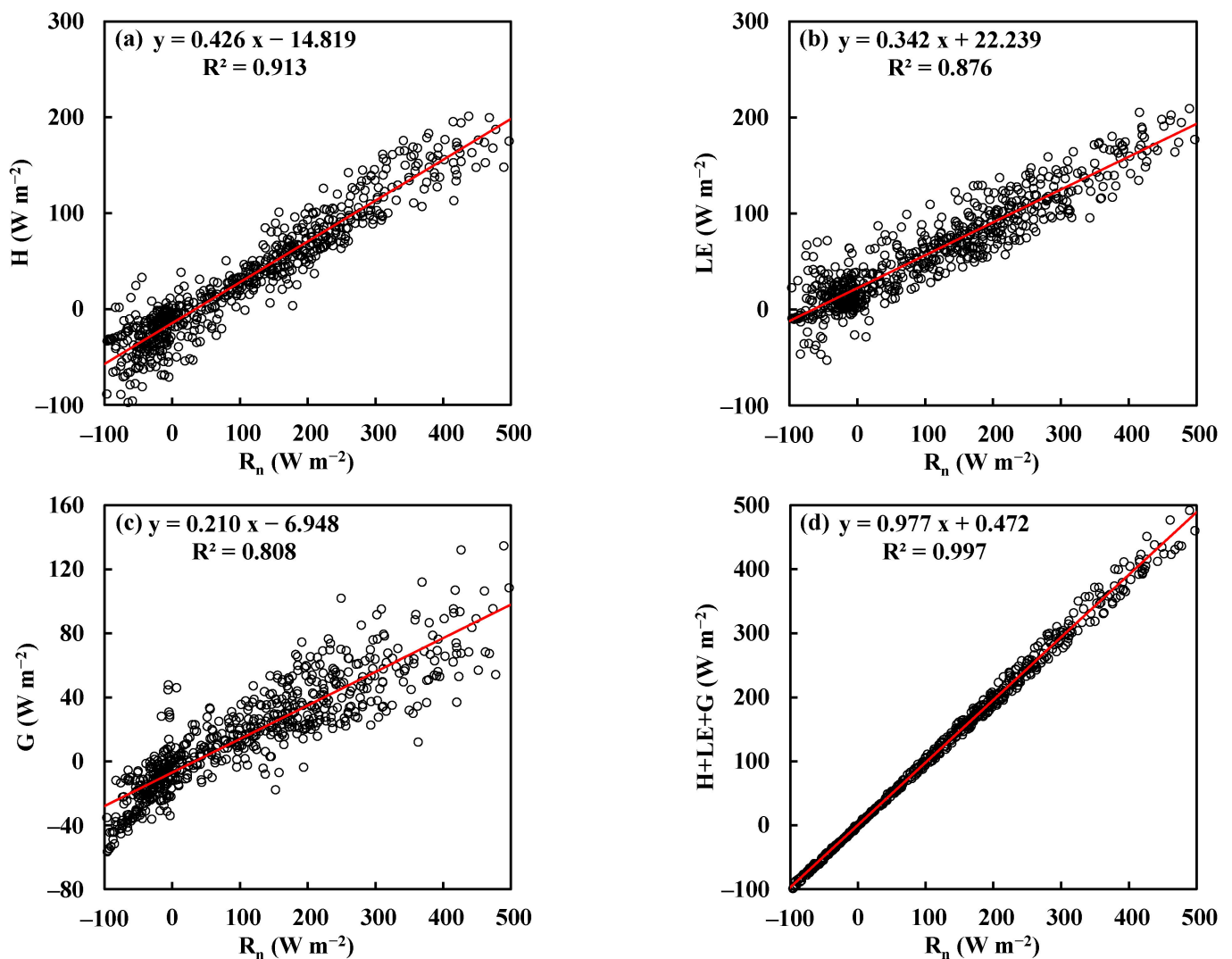


Figure 2. Scatter plots between R_n and H (a), LE (b), G (c), and $H+LE+G$ (d) above the peat bog.

2.3. Forest

This montane forest is part of the National Taiwan University Experimental Forest located in Sitou, Nantou county, central Taiwan. The area of this forest is about 2500 ha and the altitude ranges from 800 to 2000 m. Two meteorological towers (A and B; elevation around 1200 m) were built on the Japanese cedar (*Cryptomeria japonica*) forest area. The area of this *Cryptomeria* is 80 ha with an average slope of 13.6° . The average canopy height was about 26 m. The coordinates of tower A (original tower) are $23^\circ 39' 50.1''$ N, $120^\circ 47' 46.4''$ E, and 1252 m above sea level; the location of tower B (new tower) is 64 m away from tower A, and the coordinates are $23^\circ 39' 51.09''$ N, $120^\circ 47' 44.57''$ E, and 1233 m above sea level. The heights of tower A and B were 35 and 40 m, respectively. The climate of this site is warm and humid. The average annual temperature, humidity, and precipitation are $16.6^\circ C$, 89%, and 2635 mm, respectively. In this humid experimental region, fog often occurs in the afternoons in autumn and winter.

For this study, the flux data collected on tower A by the open-path EC system at 28 m above the ground was used. The EC system consisted of a three-dimensional sonic anemometer (CSAT3) and an open-path infrared gas analyzer (Li-7500). The 10 Hz analog signals were simultaneously collected by a data logger (CR3000) and were then averaged every 30 min. In addition, a net radiometer (NR-LITE) and rain gauge (TE525MM) were installed at 27.5 m to measure net radiation and precipitation. A temperature and humidity

probe (HMP45C) and a precision infrared temperature sensor (IRTS-P) were installed at 28 m to measure air temperature, relative humidity, and canopy surface temperature. All of the above sensors were connected to a data logger (CR23X). The sampling rate for these sensors was 30 s and the averaging period was 30 min. The data were collected from May 22, 2009 to July 31, 2010. The site and instrumentation features are summarized in Table 3.

Table 3. Summary of regression analysis between measured and model-predicted fluxes at the three sites. $Y = aX + b$; Y is measured flux; X is predicted flux.

Site	Model	Latent Heat Flux				Sensible Heat Flux			
		a	b	R ²	RMSE	a	b	R ²	RMSE
Grassland	P-M	0.930	18.221	0.895	28.338	0.874	−13.689	0.869	29.310
	P-T	0.884	21.336	0.922	27.362	1.039	−19.791	0.894	27.251
	N-P	0.906	23.484	0.913	29.866	0.974	−21.189	0.882	30.447
Peat Bog	P-M	0.709	9.729	0.874	32.507	1.156	7.505	0.852	29.781
	P-T	0.691	20.482	0.888	29.047	1.347	−16.744	0.896	26.967
	N-P	0.675	18.608	0.826	33.161	1.133	−1.661	0.797	31.063
Forest	P-M	0.950	−1.269	0.603	28.799	0.864	3.026	0.883	29.575
	P-T	0.687	18.383	0.643	33.945	1.185	−17.503	0.875	33.004
	N-P	0.433	35.156	0.601	66.553	1.823	−81.167	0.734	64.657

The scatter plots between R_n and H, LE, G, and H+LE+G above the forest site are shown in Figure 3. For this site, the energy partitions for H and LE were about 57% and 35%, respectively; only 4% of the energy was transported into the ground due to the high forest canopy; and the energy closure rate was 97%. These analyses for energy partitions above the forest site are also summarized in Table 2.

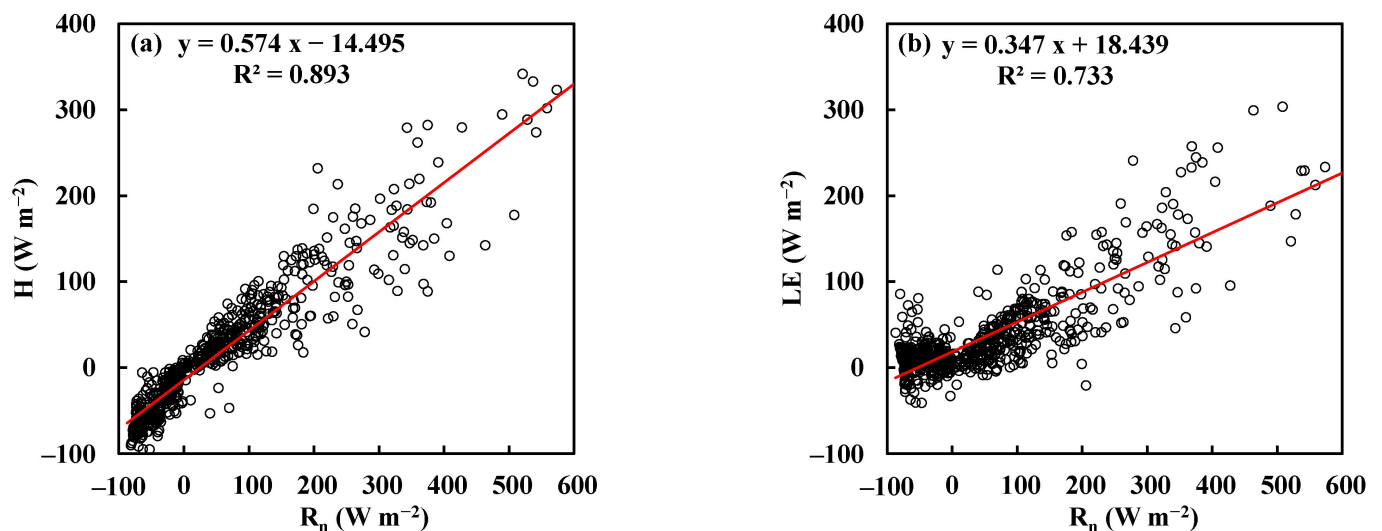


Figure 3. Cont.

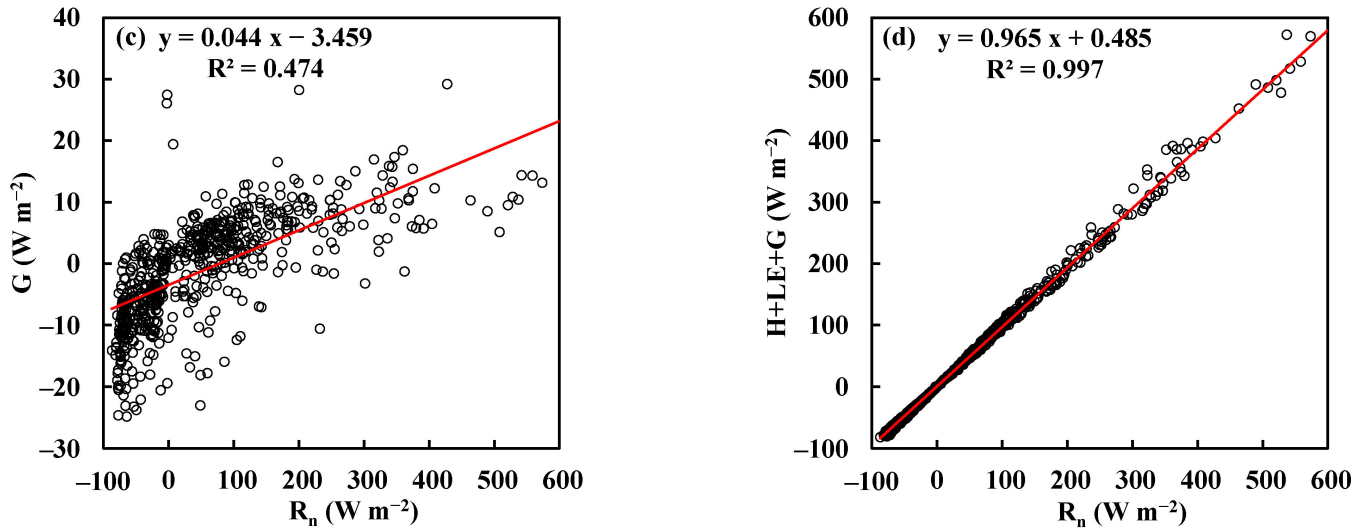


Figure 3. Scatter plots between R_n and H (a), LE (b), G (c), and $H+LE+G$ (d) above the forest.

3. Methodology

3.1. Penman–Monteith Equation

The P–M equation [3] is a widely used method for calculating water vapor flux and can be expressed as follows:

$$LE = \frac{\Delta}{\Delta + \left(1 + \frac{r_c}{r_{av}}\right)\gamma} (R_n - G) + \frac{\rho D C_p r_{av}^{-1}}{\Delta + \left(1 + \frac{r_c}{r_{av}}\right)\gamma} \quad (1)$$

where γ ($= C_p P / 0.622 L_v$) is the psychrometric constant (kPa K^{-1}), C_p is the specific heat of air ($\text{J kg}^{-1} \text{K}^{-1}$), P is the atmospheric pressure (kPa), L_v is the latent heat of evaporation (J kg^{-1}), Δ is the slope of the saturated vapor pressure (kPa K^{-1}) calculated at T_a , D is the vapor pressure deficit (kPa), r_c is the canopy resistance (s m^{-1}), and r_{av} is the aerodynamic resistance (s m^{-1}).

The aerodynamic resistance can be calculated by:

$$r_{av} = \frac{[\ln(z/z_0)][\ln(z/z_{0v})]}{k^2 U} \quad (2)$$

where k ($= 0.4$) is the von Karman constant, U is the mean wind speed (m s^{-1}), z is the measurement height, z_0 is the surface roughness for momentum ($\approx 0.1 h$, h is canopy height), and z_{0v} is the surface roughness for water vapor ($\approx 0.01 h$).

Under the framework of the P–M equation, the sensible heat flux is simply calculated by the surface energy balance equation:

$$H = R_n - G - LE \quad (3)$$

In order to apply the P–M equation, the canopy resistance must be determined (or known) a priori. In this study, data from each site were divided into two parts. The first 25% of the data was used for determining r_c . Here, the r_c value, which could result in a minimum RMSE (root mean square error) between the observed LE and the predicted LE by Equation (1), was the one adopted. The remaining 75% of the data was then used for evaluating the performance of the P–M equation with this r_c value. The determined r_c values for the grassland, peat bog, and forest sites were 60, 63, and 134 (s m^{-1}), respectively. These r_c values for the three sites are also listed in Table 1.

4.1.1. Grassland

Figure 4 shows the comparisons between the measured and model-predicted LE and H values above the grassland. The regression analyses between measured and model-predicted fluxes are also summarized in Table 3. Figure 4 and Table 3 reveal that all three of the models can predict both LE (R^2 between 0.90–0.92; RMSE around 30 W m^{-2}) and H (R^2 between 0.87–0.89; RMSE around 30 W m^{-2}) accurately above the grassland site.

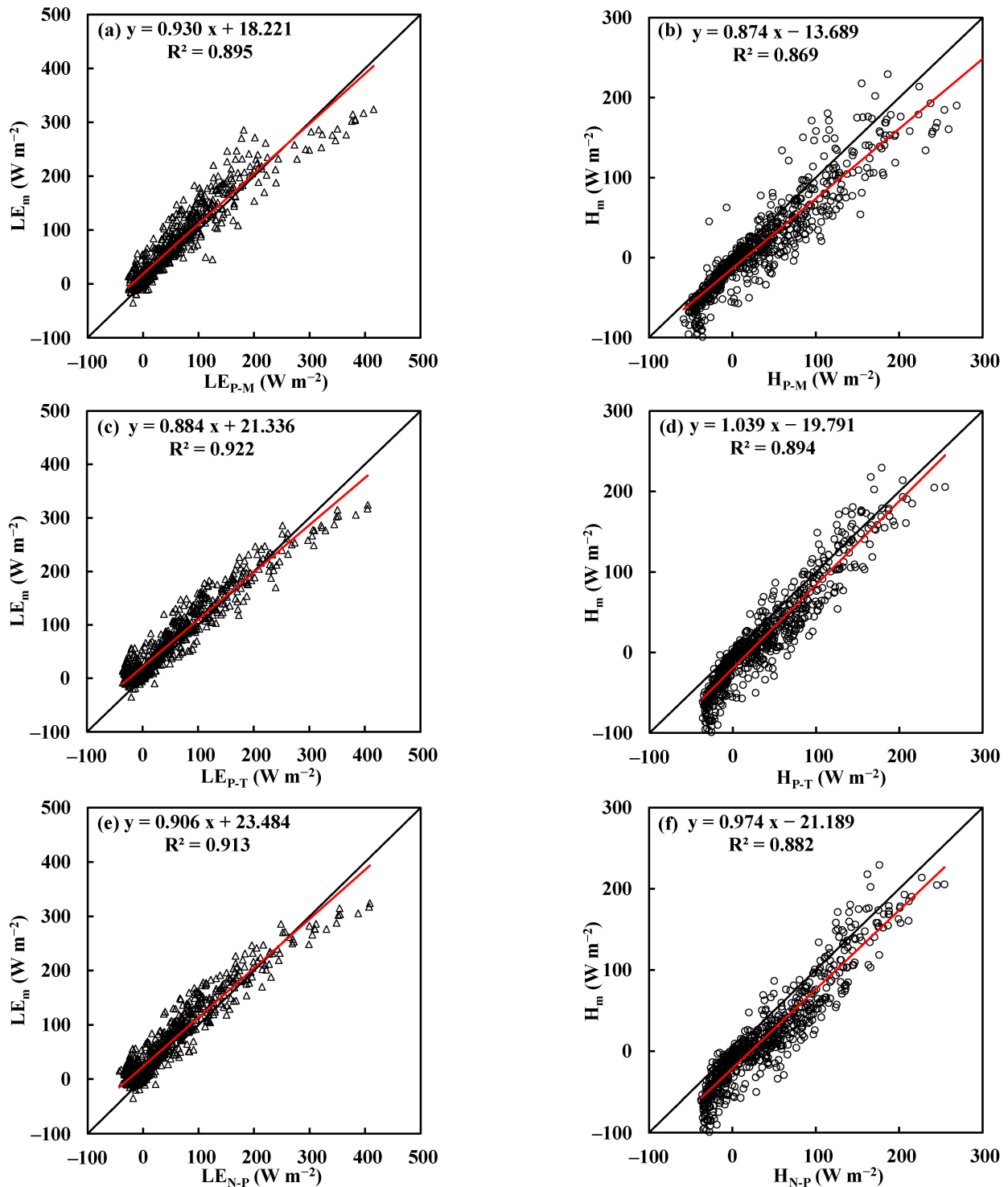


Figure 4. Comparisons of measured and predicted LE and H by the P–M equation (a,b), P–T equation (c,d), and N–P method (e,f) above the grassland. The 1:1 line is also shown.

To further examine model performance, we plotted the measured and model-predicted LE and H values as a function of available energy ($R_n - G$) at the grassland, as shown in Figure 5. For the cases of low available energy ($R_n - G < 300$), all three models resulted in similar and slightly underestimated LE values. This indicated that the actual evapotranspiration rate was slightly higher than the equilibrium evaporation rate when the available energy was small. This extra evapotranspiration was due to the demand of unsaturated atmosphere.

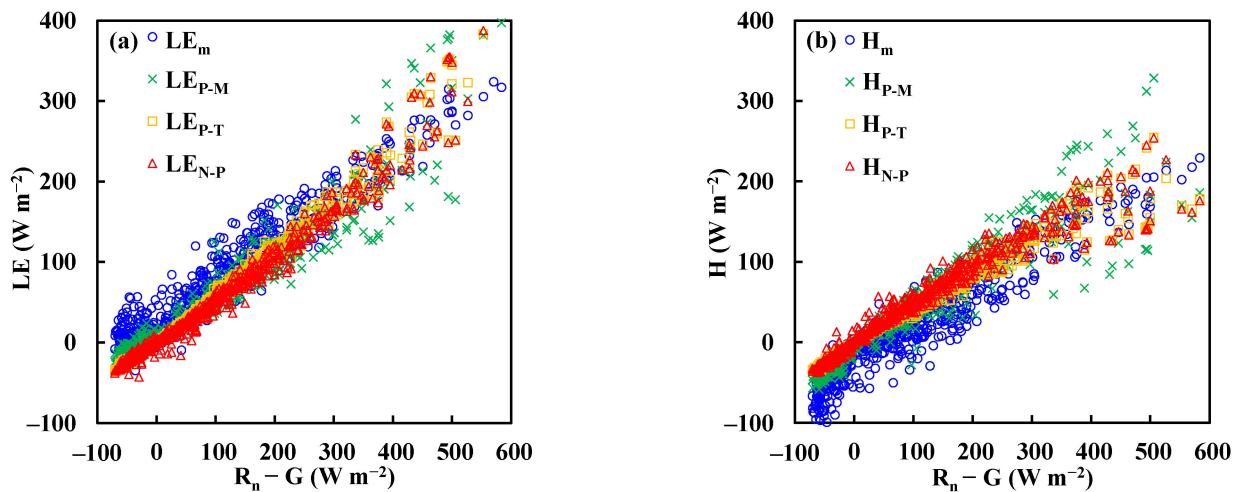


Figure 5. Scatter plots of measured and model-predicted LE (a) and H (b) as a function of available energy ($R_n - G$) above the grassland.

4.1.2. Peat Bog

The comparisons between measured and model-predicted LE and H above the peat bog are shown in Figure 6. The regression analyses between measured and model-predicted fluxes are also listed in Table 3. From Figure 6 and Table 3, it is clear that all of the LE predictions from the three models are in agreement with the measurements (R^2 between 0.82–0.89); similar results are also found for H (R^2 between 0.79–0.90). The RMSEs for LE (between 29–33 $W m^{-2}$) and H (between 27–31 $W m^{-2}$) for each of the models are approximately the same as those at the grassland site. Overall, these three models performed well above the peat bog site.

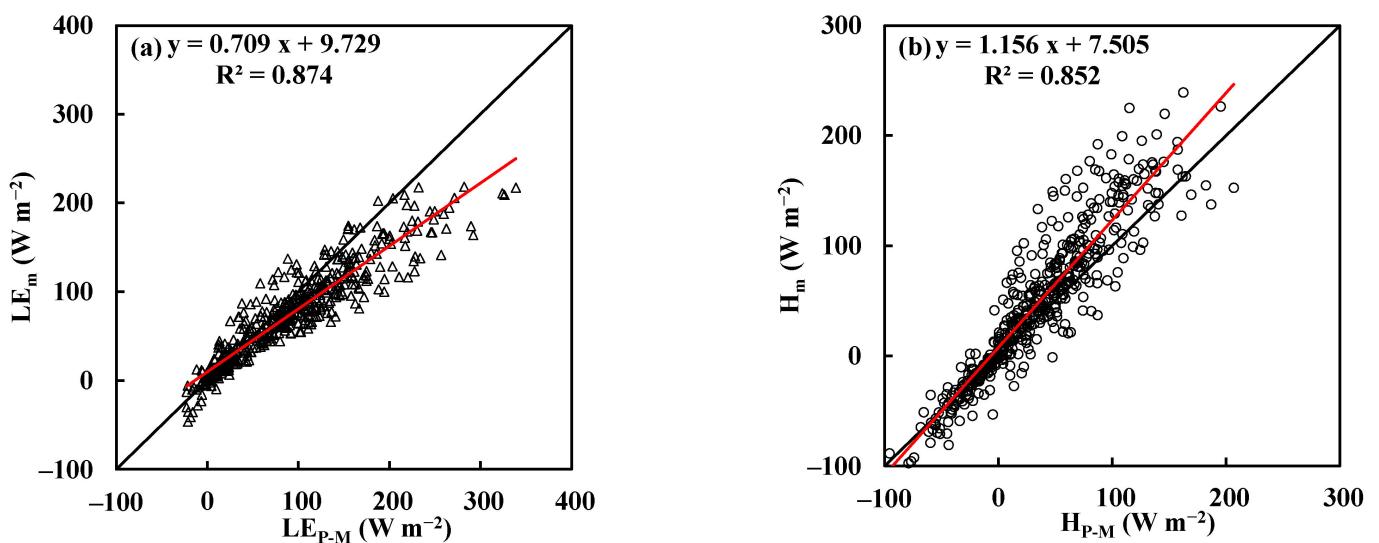


Figure 6. Cont.

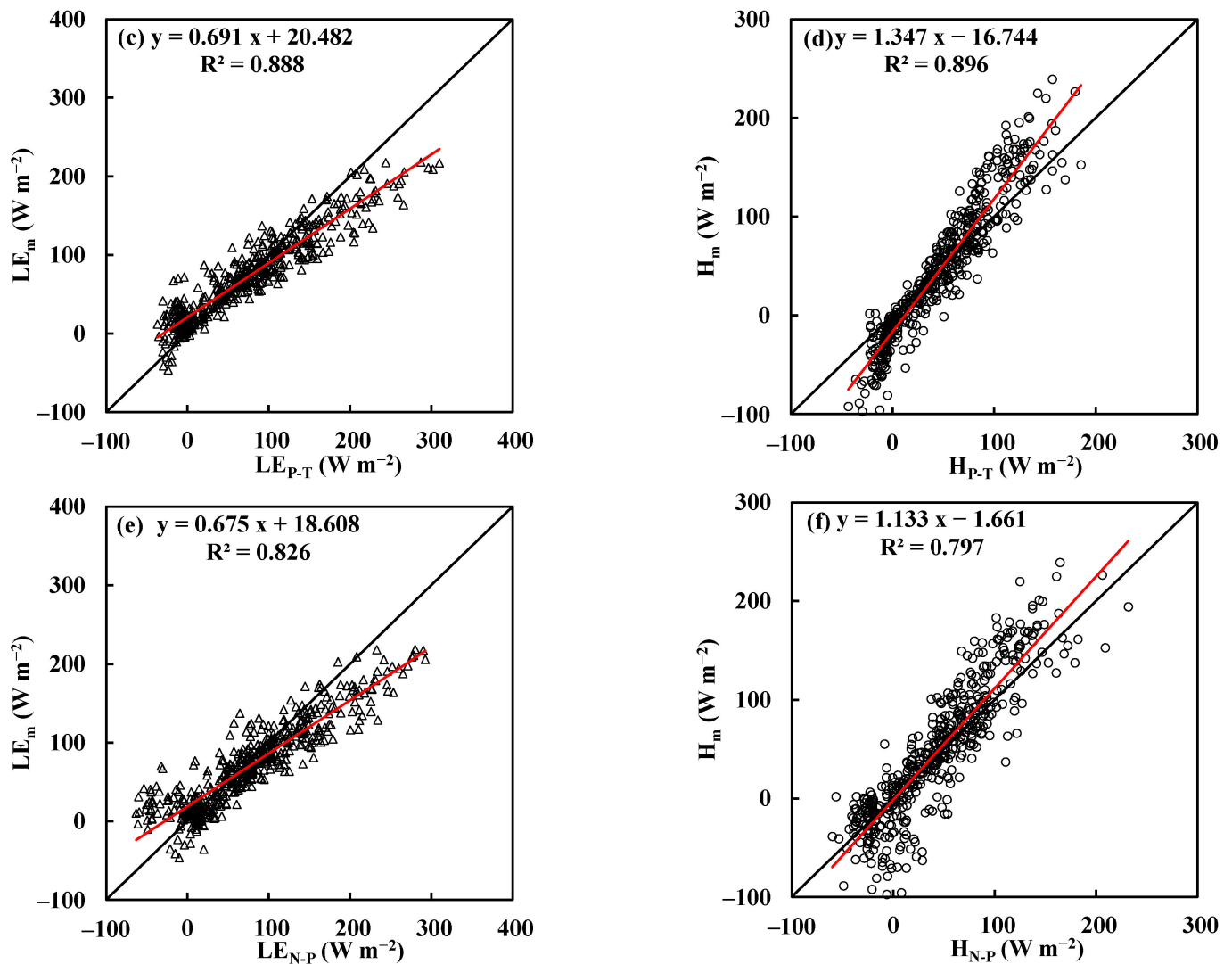


Figure 6. Comparisons of measured and predicted LE and H by the P-M equation (a,b), P-T equation (c,d), and non-parametric method (e,f) above the peat bog. The 1:1 line is also shown.

Further model performance evaluation was done by plotting the measured and model-predicted LE and H values as a function of available energy ($R_n - G$) at the peat bog (Figure 7). From Figure 7 it appears for the cases of high available energy ($R_n - G > 300$), all three of the models slightly overpredicted LE. This shows that the actual evapotranspiration rate was slightly lower than the equilibrium evaporation rate when the available energy was large. This reduction of evapotranspiration might have been caused by resistance from the vegetation in order to reduce water loss during higher air temperature and radiation.

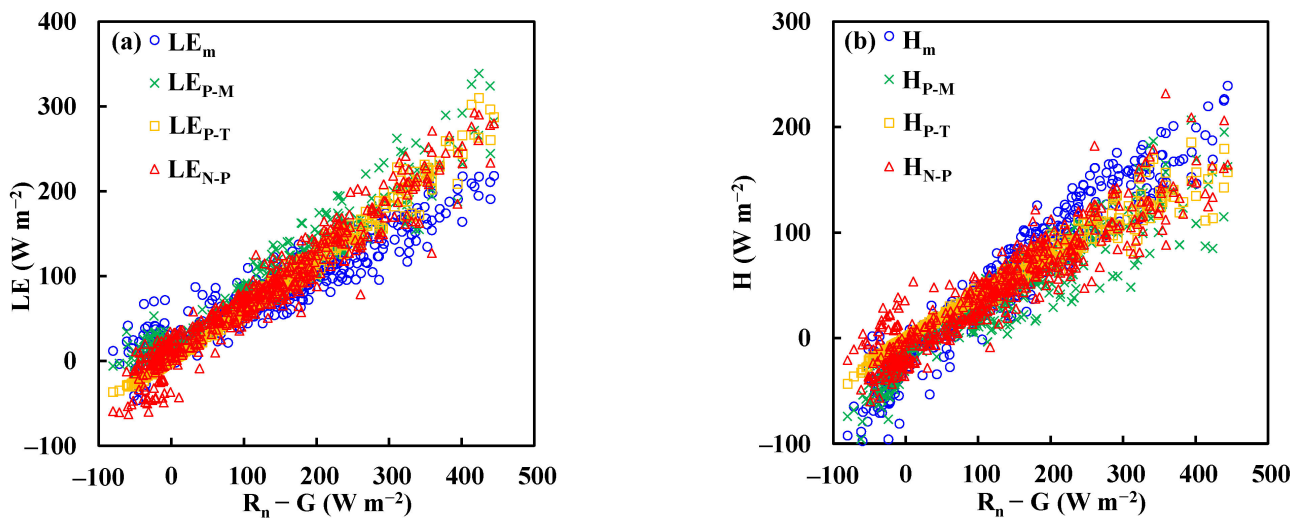


Figure 7. Scatter plots of measured and model-predicted LE (a) and H (b) as a function of available energy ($R_n - G$) above the peat bog.

4.1.3. Forest

The scatter plots of measured and model-predicted LE and H above the forest are shown in Figure 8. The regression analyses between measured and model predicted fluxes are also listed in Table 3. From Figure 8 and Table 3, both the P–M and P–T equations appear to have reproduced LE and H accurately (RMSEs around 30 W m^{-2}) above the forest site. However, the LE and H predicted by the N–P method were not in agreement with the measurements (both RMSEs were around 65 W m^{-2}).

Figure 9 shows the measured and model-predicted LE and H values as a function of available energy ($R_n - G$) at the forest site. In Figure 9, it appears that in the cases of high available energy ($R_n - G > 400$), the N–P method overpredicted LE and underestimated H. This reveals that the actual evapotranspiration rate was much lower than the equilibrium evaporation rate when the available energy was large. Similar to the peat bog site (although the magnitude was larger), this reduction of evapotranspiration might have been caused by resistance from the vegetation in order to avoid a large amount of water loss (physiological control) during high air temperature and radiation.

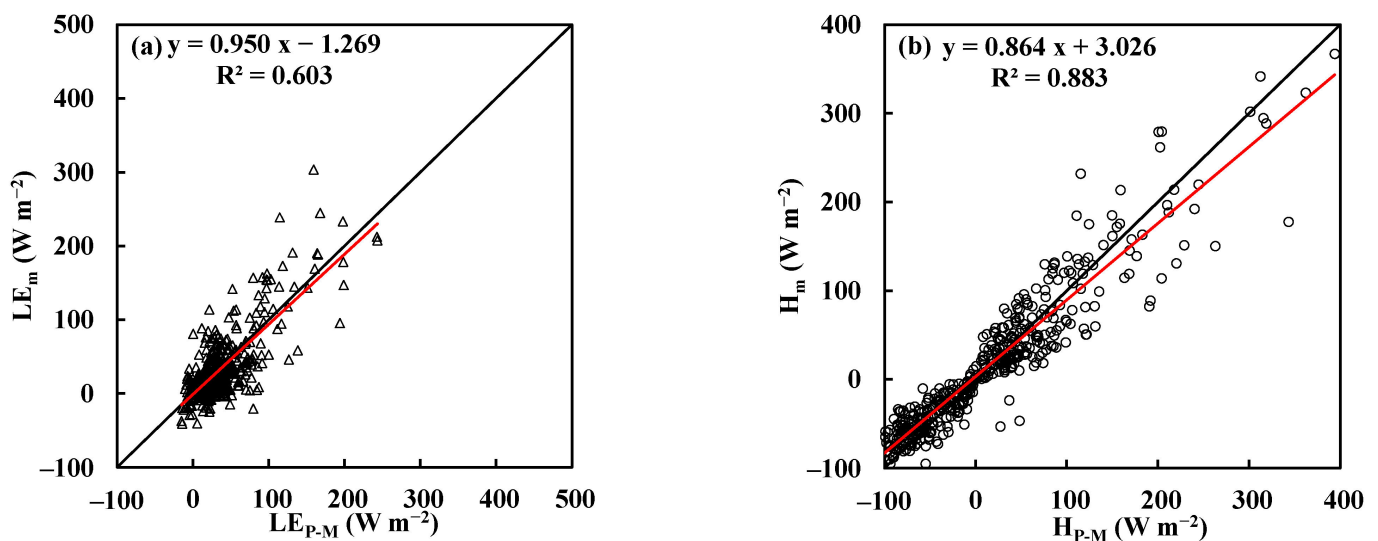


Figure 8. Cont.

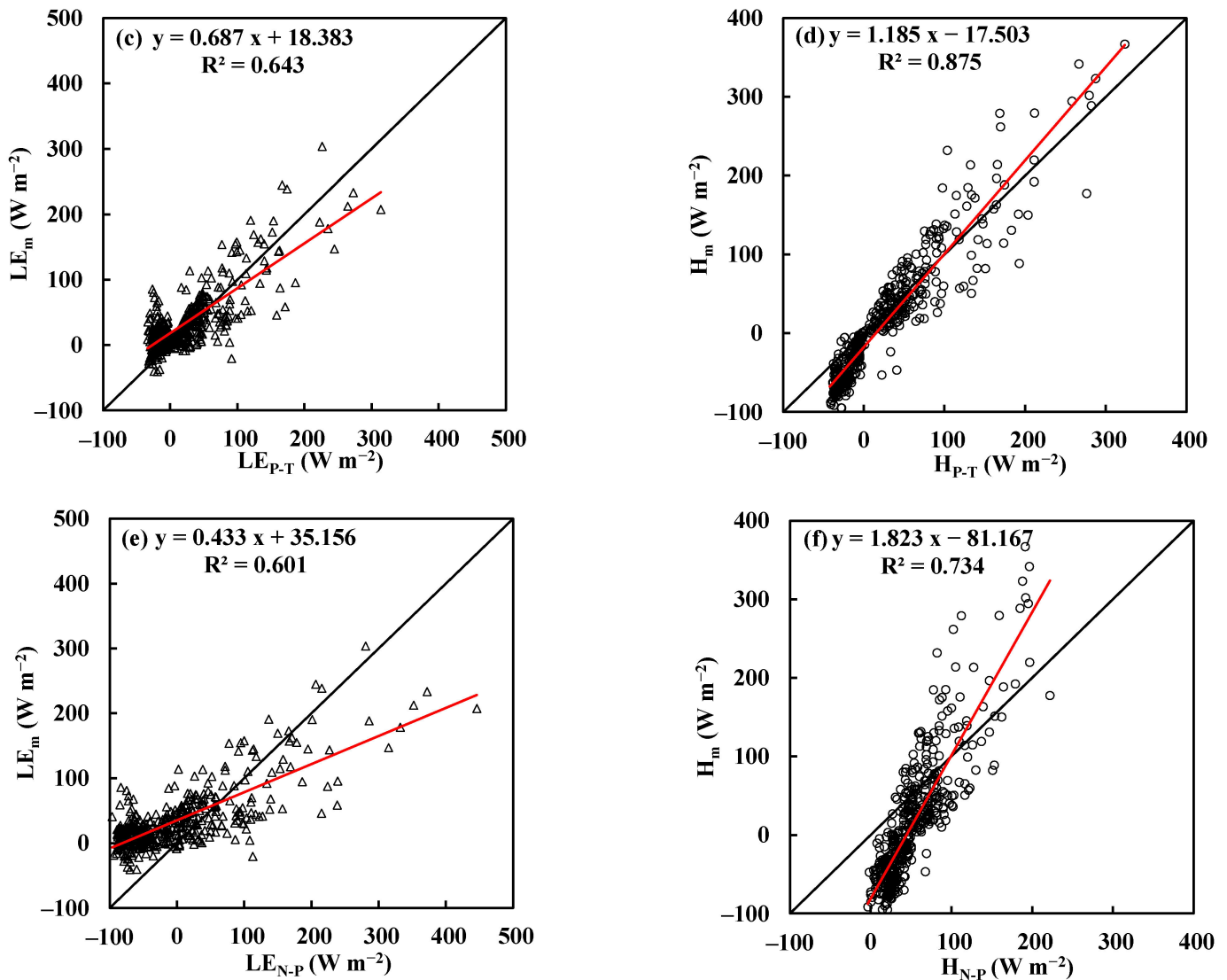


Figure 8. Comparisons of measured and predicted LE and H by the P-M equation (a,b), P-T equation (c,d), and non-parametric method (e,f) above the forest. The 1:1 line is also shown.

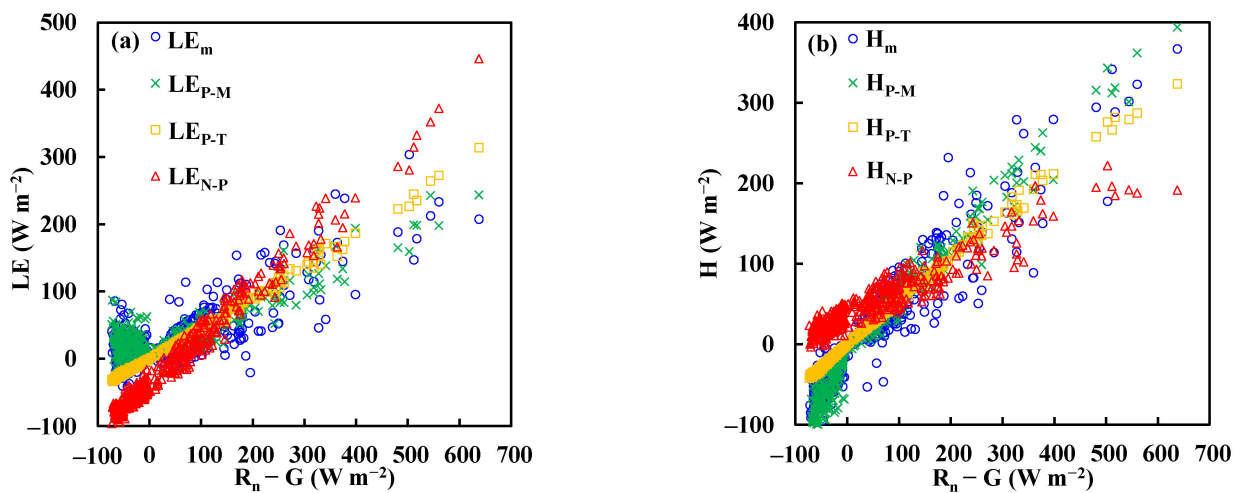


Figure 9. Scatter plots of measured and model-predicted LE (a) and H (b) as a function of available energy ($R_n - G$) above the forest.

4.2. Limitation of the Non-Parametric Method

To further investigate the limitation and accuracy of the non-parametric method, in this section we analyze the contribution of each term in the N-P method.

Figure 10 plots the three terms in the non-parametric method as a function of $R_n - G$ for latent heat and sensible heat fluxes above the grassland, peat bog, and forest. For all three sites, term III is very small and close to zero. Hence, term III can be neglected.

Using the P-T equation and replacing LE with αLE_{eq} in Equation (6), and neglecting term III, we have

$$\text{term II} = (1 - \alpha)LE_{eq} \tag{7}$$

Now by replacing LE_{eq} with LE/α in Equation (6), we get

$$\text{term II} = \left(\frac{1}{\alpha} - 1\right)LE \tag{8}$$

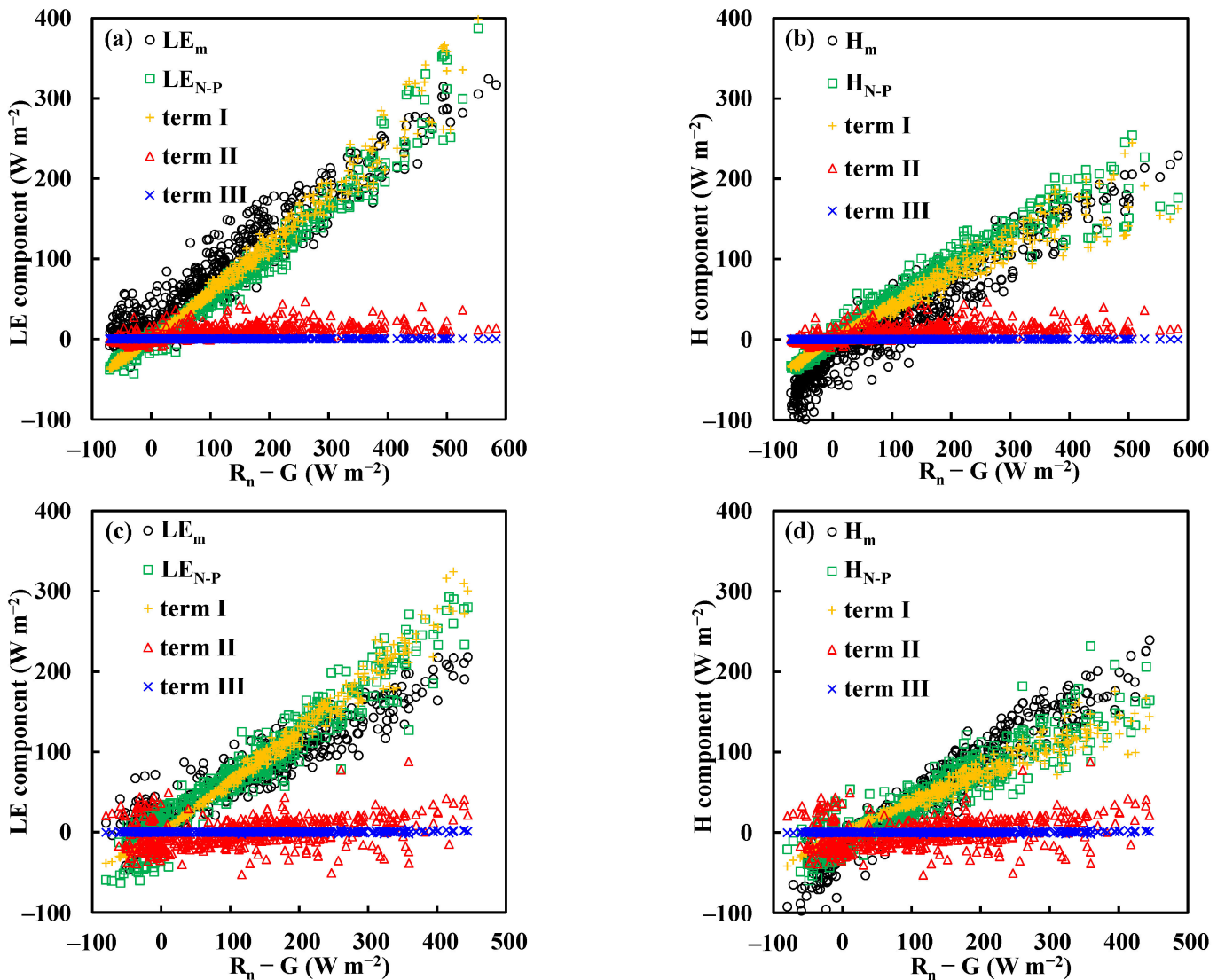


Figure 10. Cont.

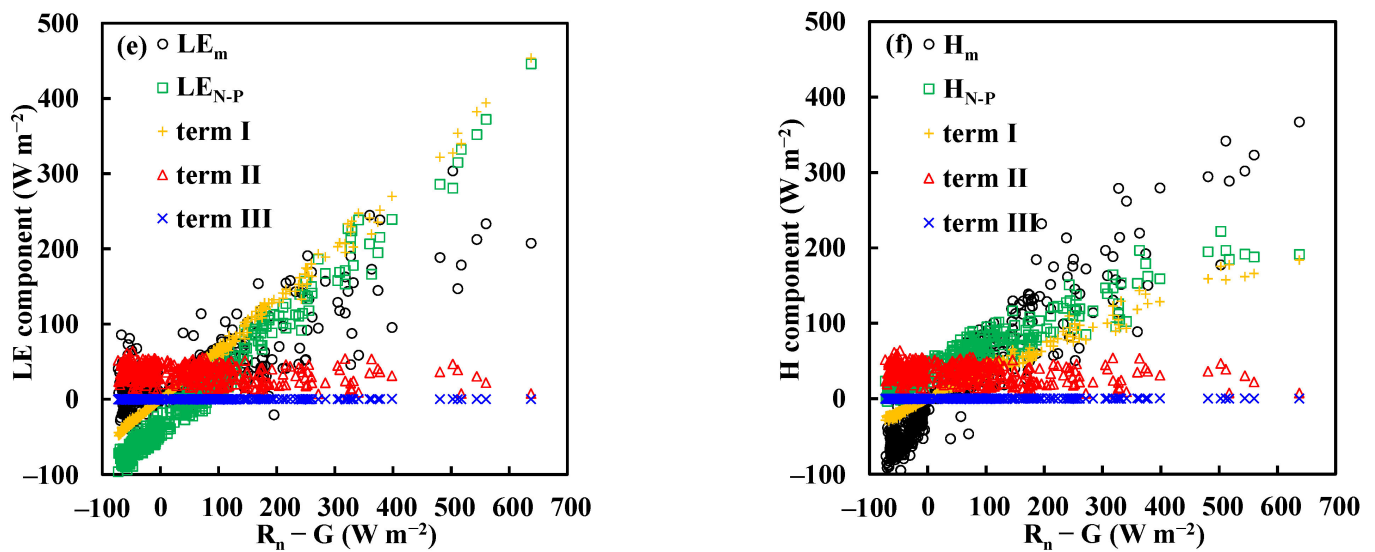


Figure 10. Scatter plots of the three terms in the non-parametric method as a function of $R_n - G$ for LE and H above the grassland (a,b), peat bog (c,d), and forest (e,f).

Equations (7) or (8) represent the condition that should be satisfied if the N-P method is applied for estimating LE. Figure 11 shows the relationship between term II and LE_{eq} along with the measured LE for the three sites. In Figure 11, the slopes for the grassland and peat bog sites are positive, but those for the forest site are negative. This is because when R_n for the forest site is large, most of the energy (57%, see Table 2) is distributed to H for warming up the air; hence, the difference between T_s and T_a is reduced which results in a smaller term II. Figure 11 also reveals that term II is about $\pm 10\%$ (from -0.051 to 0.083) of the equilibrium evapotranspiration (Figure 11a,c,e).

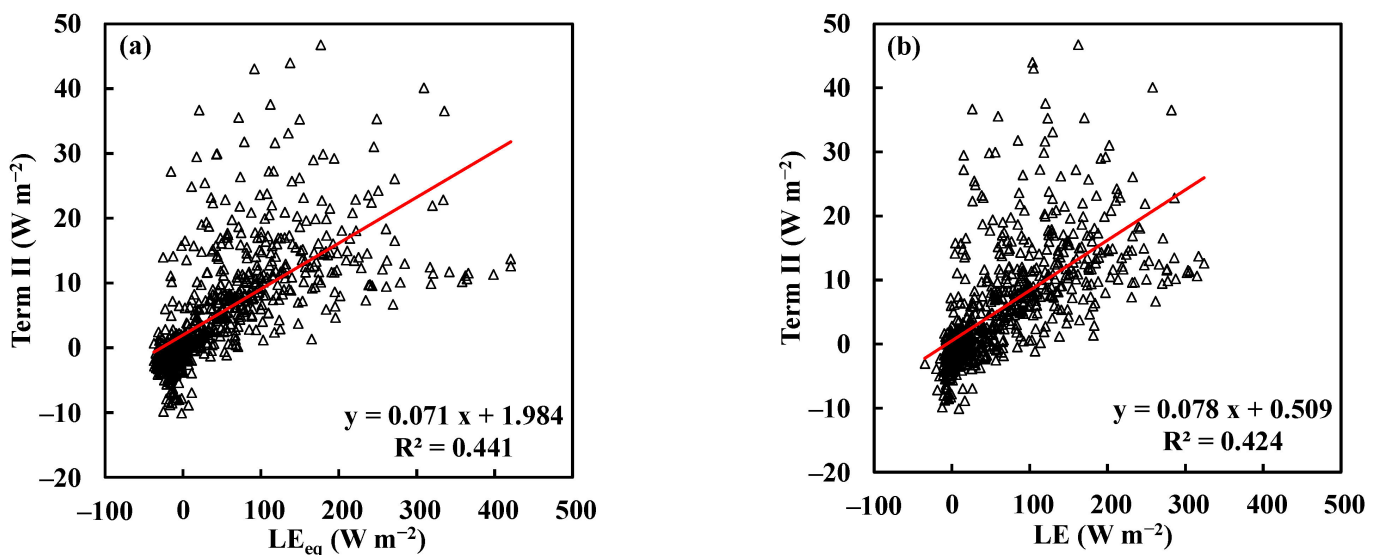


Figure 11. Cont.

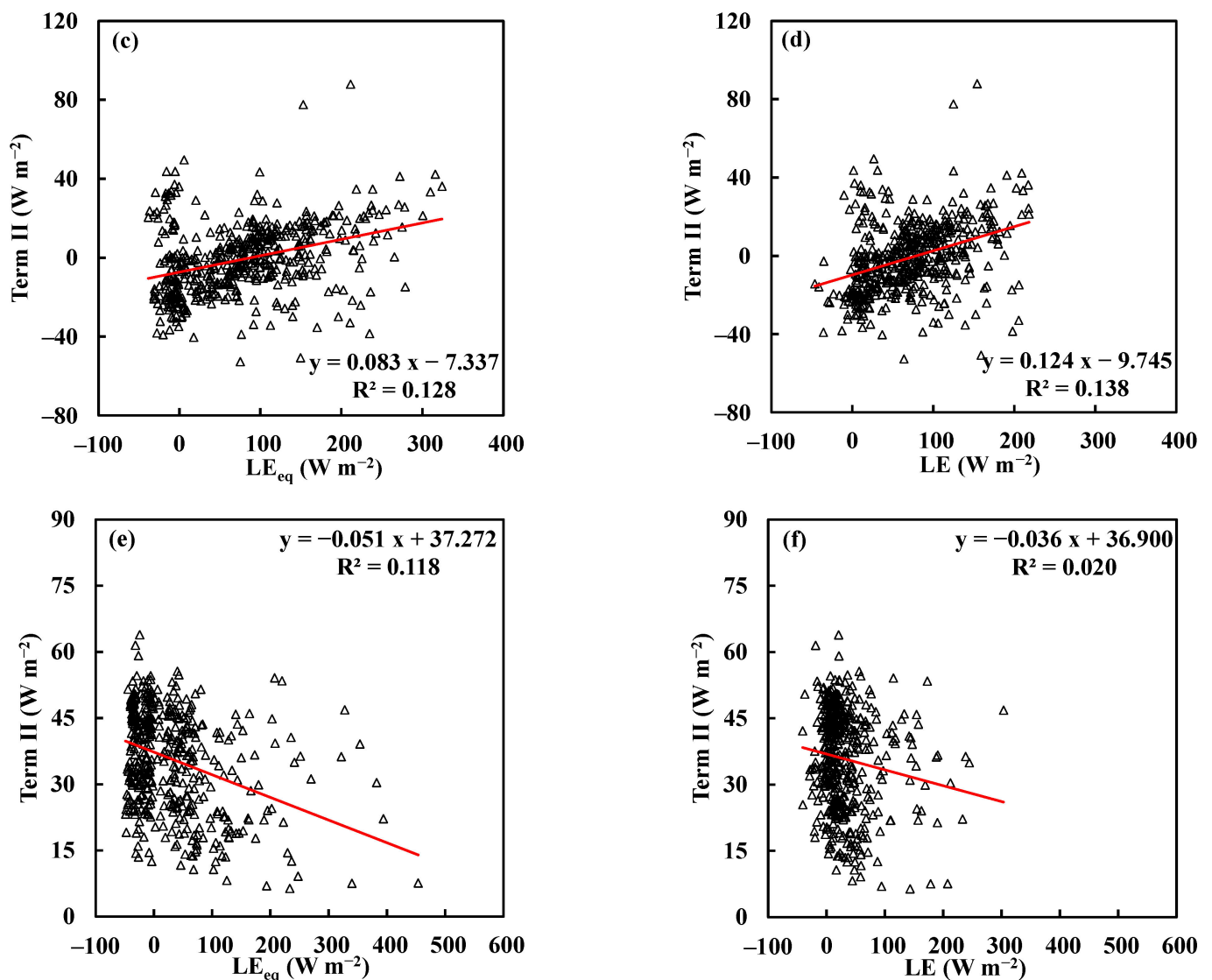


Figure 11. Scatter plots of term II as a function of LE_{eq} and measured LE above the grassland (a,b), peat bog (c,d), and forest (e,f).

From the linear regression analyses shown in Figure 11 and Equations (7) and (8), we found that the α values for the three sites ranged from 0.89–1.05 (see Table 4). This means that when applying the N-P method to estimate LE, the actual evapotranspiration should be around 0.89–1.05 times the equilibrium evapotranspiration. Both the grassland and peat bog sites met this condition (both $\alpha = 0.96$). However, the P-T constant at the forest is only 0.69; hence, Equations (7) and (8) are not satisfied. This explains why the N-P method performed well for the grassland and peat bog, but not so well for the forest.

Table 4. α derived from Equations (7) and (8).

Site	Grassland	Peat Bog	Forest
α from Equation (7)	0.929	0.917	1.051
α from Equation (8)	0.928	0.890	1.037

The N-P method assumes that “the system of liquid water in leaf tissues and the water vapor in the atmosphere tends to evolve towards a potential equilibrium as quickly as possible by maximization of the transpiration rate” [29]; however, a system like the forest,

which tends to reduce the transpiration rate during high air temperature and radiation in order to avoid a large amount of water loss, would violate this assumption and the N-P method is not suitable for this kind of ecosystem. As previously mentioned, the α values of the spruce forest and Scots Pine forest in dry conditions are 0.74 and 0.64, respectively [28]. This implies that the N-P method is not suitable for these forests either.

4.3. Sensitivity of the N-P Method on Surface Temperature

The advantage of the N-P method is that experimental parameters (such as r_c and α) are not needed. However, compared with the P-M and P-T equations, this method requires one additional input, T_s . Hence, it is worth noting the sensitivity of the N-P method to the change of T_s .

Taking the derivatives of H (Equation (5)) and LE (Equation (6)) with respect to T_s , we have

$$\partial H/\partial T_s = 4\varepsilon\sigma T_s^3 - G/T_s \tag{9}$$

$$\partial LE/\partial T_s = -4\varepsilon\sigma T_s^3 + G/T_s \tag{10}$$

Equations (9) and (10) describe how predicted H and LE are changed with a unit change of T_s . From Equation (10), it is clear that $\partial LE/\partial T_s$ is a function of T_s and G. From field measurements of the three sites, T_s is in the range of -5 to 30 °C, and G is between -20 and 100 ($W\ m^{-2}$). From these conditions, with $\varepsilon = 0.95$, Figure 12 plots $\partial LE/\partial T_s$ and $\partial H/\partial T_s$ as a function of T_s under different G values. Figure 12 reveals that with a one-degree change in T_s , the predicted LE and H are only changed by 4 to 6 ($W\ m^{-2}$). In other words, the LE predicted by the N-P method is not sensitive to the uncertainty of T_s measurements.

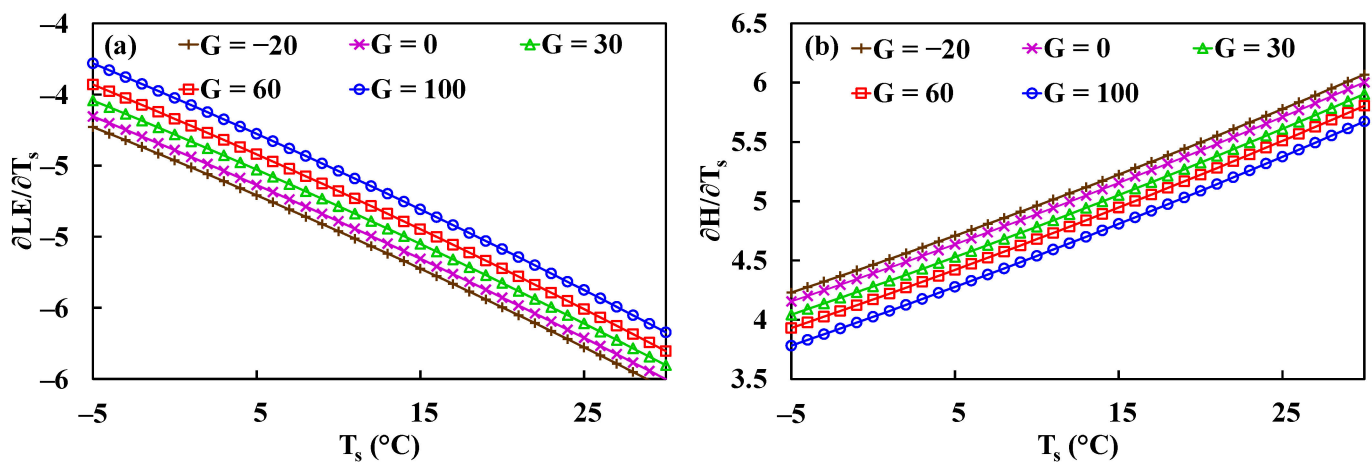


Figure 12. (a) $\partial LE/\partial T_s$, (b) $\partial H/\partial T_s$ as a function of T_s under different ground heat flux.

5. Conclusions

Field measurements above grassland, peat bog, and forest were used to investigate the accuracy and limitations of the non-parametric method in predicting evapotranspiration. The model’s performance was also compared with those of the Penman–Monteith and Priestley–Taylor equations. Our results demonstrate the following:

- (1) The evapotranspiration rates above the grassland and peat bog were close to the equilibrium evaporation (P-T constant ≈ 0.96). The forest’s evapotranspiration rate was 69% of the equilibrium evaporation, and about 60% of the net radiation energy was distributed to sensible heat flux.
- (2) Both the P-M and P-T equations performed well at estimating water vapor and sensible heat fluxes for all of the three sites. However, the canopy resistance in the P-M equation and the Priestley–Taylor constant in the P-T equation must be known a priori.

- (3) The water vapor flux predictions by the N-P method were in agreement with the measurements above the grassland and peat bog. However, this was not the case for the forest site.
- (4) Our analysis shows that with one degree of change in T_s , the predicted LE is only changed by 4 to 6 ($W m^{-2}$). Hence, the LE predictions by the N-P method are not sensitive to the uncertainty of T_s measurements.
- (5) Field measurements from the three sites reveal that the second term of the N-P method is about $\pm 10\%$ (from -0.05 to 0.08) of the equilibrium evapotranspiration. For applying the N-P method to estimate LE, the actual evapotranspiration of the site should be around 0.89–1.05 times the equilibrium evapotranspiration.

In theory, the non-parametric method assumes that at the local thermal equilibrium environment (i.e., $T_a = T_s$), the actual evaporation rate is the equilibrium evaporation, and that when the surface temperature is increased (i.e., $T_s > T_a$), the actual evaporation rate will be dropped since some energy is used for sensible heat flux. Our field measurements show that this energy adjustment is small (around 10% of LE_{eq}). Hence, the N-P method is only suitable for a system where the actual evaporation rate is close to the equilibrium evaporation (difference within $\pm 10\%$). For a system (such as the forest) where the actual LE is much less than LE_{eq} , this method will not work.

Author Contributions: C.-I.H. conceived the research idea; C.-I.H., C.-J.C., and I.-H.H. performed the model simulations; G.K. performed the grassland and peat bog experiments; C.-I.H. performed the forest experiment; all authors took part in the discussion, data analysis, and interpretation of the data and model predictions; C.-I.H., C.-J.C., and I.-H.H. wrote the manuscript. All authors reviewed the manuscript. All authors have read and agreed to the published version of the manuscript.

Funding: This work was supported, in part, by the Ministry of Science and Technology, Taiwan [grant number: MOST 110-2111-M-002-011] and the Core Research Project, National Taiwan University [project number: NTU-CC-110L890903; NTU-CC-111L890903].

Data Availability Statement: The data used to support the findings of this study are available from the corresponding author upon request.

Acknowledgments: The authors are grateful to Shih-Min Cheng for her great help with the forest experiment.

Conflicts of Interest: The authors declare no conflict of interest.

Abbreviations

Symbol	Description
C_p	specific heat of air ($J kg^{-1} K^{-1}$)
D	vapor pressure deficit (kPa)
G	ground heat flux ($W m^{-2}$)
H	sensible heat flux ($W m^{-2}$)
k	von Karman constant (= 0.4)
LE	latent heat flux ($W m^{-2}$)
L_v	latent heat of evaporation ($J kg^{-1}$)
P	atmospheric pressure (kPa)
R_n	net radiation ($W m^{-2}$)
r_c	canopy resistance ($s m^{-1}$)
r_{av}	aerodynamic resistance ($s m^{-1}$)
T_a	air temperature ($^{\circ}C$)
T_s	surface temperature ($^{\circ}C$)
U	wind speed ($m s^{-1}$)
z	measurement height (m)
z_o	surface roughness for momentum (m)
z_{ov}	surface roughness for water vapor (m)

α	Priestly–Taylor constant
γ	psychrometric constant (kPa K ⁻¹)
Δ	slope of the saturated vapor pressure (kPa K ⁻¹)
ε	land surface emissivity
σ	Stefan–Boltzmann constant ($= 5.67 \times 10^{-8}$) (W m ⁻² K ⁻⁴)

References

- Liu, Y.; Hiyama, T.; Yasunari, T.; Tanaka, H. A nonparametric approach to estimating terrestrial evaporation: Validation in eddy covariance sites. *Agric. For. Meteorol.* **2012**, *157*, 49–59. [[CrossRef](#)]
- Shuttleworth, W.J. Putting the “vap” into evaporation. *Hydrol. Earth Syst. Sci.* **2007**, *11*, 210–244. [[CrossRef](#)]
- Monteith, J.L. Evaporation and surface temperature. *Q. J. R. Meteor. Soc.* **1981**, *107*, 1–27. [[CrossRef](#)]
- Raupach, M.R. Influences of local feedbacks on land–air exchanges of energy and carbon. *Glob. Change Biol.* **1998**, *4*, 477–494. [[CrossRef](#)]
- Irmak, S.; Mutiibwa, D. On the dynamics of canopy resistance: Generalized linear estimation and relationships with primary micrometeorological variables. *Water Resour. Res.* **2010**, *46*, 8. [[CrossRef](#)]
- Lin, B.S.; Lei, H.; Hu, M.C.; Visessri, S.; Hsieh, C.I. Canopy resistance and estimation of evapotranspiration above a humid cypress forest. *Adv. Meteorol.* **2020**, *2020*, 4232138. [[CrossRef](#)]
- Priestley, C.H.B.; Taylor, R.J. On the assessment of surface heat flux and evaporation using large-scale parameters. *Mon. Weather Rev.* **1972**, *100*, 81–92. [[CrossRef](#)]
- Pereira, A.R. The Priestley–Taylor parameter and the decoupling factor for estimating reference evapotranspiration. *Agric. For. Meteorol.* **2004**, *125*, 305–313. [[CrossRef](#)]
- Bottazzi, M.; Bancheri, M.; Mobilia, M.; Bertoldi, G.; Longobardi, A.; Rigon, R. Comparing evapotranspiration estimates from the geoframe-prospere model with Penman–Monteith and Priestley–Taylor approaches under different climate conditions. *Water* **2021**, *13*, 1221. [[CrossRef](#)]
- Qiu, R.J.; Liu, C.W.; Cui, N.B.; Wu, Y.J.; Wang, Z.C.; Li, G. Evapotranspiration estimation using a modified Priestley–Taylor model in a rice–wheat rotation system. *Agric. Water Manag.* **2019**, *224*, 105755. [[CrossRef](#)]
- Magyari, E.; Keller, B. Hamiltonian description of the heat conduction. *Heat Mass Transf.* **1999**, *34*, 453–459. [[CrossRef](#)]
- Pan, X.; Liu, Y.; Fan, X. Satellite retrieval of surface evapotranspiration with nonparametric approach: Accuracy assessment over a semiarid region. *Adv. Meteorol.* **2016**, *2016*, 1584316. [[CrossRef](#)]
- Pan, X.; Liu, Y.; Gan, G.; Fan, X.; Yang, Y. Estimation of evapotranspiration using a nonparametric approach under all sky: Accuracy evaluation and error analysis. *IEEE J. Sel. Top. Appl. Earth Obs. Remote Sens.* **2017**, *10*, 2528–2539. [[CrossRef](#)]
- Pan, X.; You, C.; Liu, Y.; Shi, C.; Han, S.; Yang, Y.; Hu, J. Evaluation of satellite-retrieved evapotranspiration based on a nonparametric approach over an arid region. *Int. J. Remote Sens.* **2020**, *41*, 7605–7623. [[CrossRef](#)]
- Wu, B.; Zhu, W.; Yan, N.; Xing, Q.; Xu, J.; Ma, Z.; Wang, L. Regional actual evapotranspiration estimation with land and meteorological variables derived from multi-source satellite data. *Remote Sens.* **2020**, *12*, 332. [[CrossRef](#)]
- Yang, Y.; Su, H.; Qi, J. A critical evaluation of the nonparametric approach to estimate terrestrial evaporation. *Adv. Meteorol.* **2016**, *2016*, 5343718. [[CrossRef](#)]
- Jaksic, V.; Kiely, G.; Albertson, J.; Oren, R.; Katul, G.; Leahy, P.; Byrne, K.A. Net ecosystem exchange of grassland in contrasting wet and dry years. *Agric. Forest. Meteorol.* **2006**, *139*, 323–334. [[CrossRef](#)]
- Lawton, D.; Leahy, P.; Kiely, G.; Byrne, K.A.; Calanca, P. Modeling of net ecosystem exchange and its components for a humid grassland ecosystem. *J. Geophys. Res. Biogeosciences* **2006**, *111*, G04013. [[CrossRef](#)]
- Byrne, K.A.; Kiely, G.; Leahy, P. CO₂ fluxes in adjacent new and permanent temperate grasslands. *Agric. For. Meteorol.* **2005**, *135*, 82–92. [[CrossRef](#)]
- Peichl, M.; Leahy, P.; Kiely, G. Six-year stable annual uptake of carbon dioxide in intensively managed humid temperate grassland. *Ecosystems* **2011**, *14*, 112–126. [[CrossRef](#)]
- Lewis, C.; Albertson, J.; Xu, X.; Kiely, G. Spatial variability of hydraulic conductivity and bulk density along a blanket peatland hillslope. *Hydrol. Process.* **2012**, *26*, 1527–1537. [[CrossRef](#)]
- Laine, A.; Sottocornola, M.; Kiely, G.; Byrne, K.A.; Wilson, D.; Tuittila, E.S. Estimating net ecosystem exchange in a patterned ecosystem: Example from blanket bog. *Agric. For. Meteorol.* **2006**, *138*, 231–243. [[CrossRef](#)]
- Sottocornola, M.; Laine, A.; Kiely, G.; Byrne, K.A.; Tuittila, E.S. Vegetation and environmental variation in an Atlantic blanket bog in South-western Ireland. *Plant Ecol.* **2009**, *203*, 69–81. [[CrossRef](#)]
- Sottocornola, M.; Kiely, G. Hydro-meteorological controls on the CO₂ exchange variation in an Irish blanket bog. *Agric. For. Meteorol.* **2010**, *150*, 287–297. [[CrossRef](#)]
- McVeigh, P.; Sottocornola, M.; Foley, N.; Leahy, P.; Kiely, G. Meteorological and functional response partitioning to explain interannual variability of CO₂ exchange at an Irish Atlantic blanket bog. *Agric. For. Meteorol.* **2014**, *194*, 8–19. [[CrossRef](#)]
- Gong, X.; Qiu, R.; Ge, J.; Bo, G.; Ping, Y.; Xin, Q.; Wang, S. Evapotranspiration partitioning of greenhouse grown tomato using a modified Priestley–Taylor model. *Agric. Water Manag.* **2021**, *247*, 106709. [[CrossRef](#)]
- Eichinger, W.E.; Parlange, M.B.; Stricker, H. On the concept of equilibrium evaporation and the value of the Priestley–Taylor coefficient. *Water Resour. Res.* **1996**, *32*, 161–164. [[CrossRef](#)]

-
28. Shuttleworth, W.J.; Calder, I.R. Has the Priestley-Taylor Equation Any Relevance to Forest Evaporation? *J. Appl. Meteorol.* **1979**, *18*, 639–646. [[CrossRef](#)]
 29. Wang, J.; Bras, R.L.; Lerdau, M.; Salvucci, G.D. A maximum hypothesis of transpiration. *J. Geophys. Res. Biogeosciences* **2007**, *112*, W03010. [[CrossRef](#)]